MET.O.14

METEOROLOGICAL OFFICE
BOUNDARY LAYER RESEARCH BRANCH
TURBULENCE & DIFFUSION NOTE

T.D.N. No. 85

Direct measurements of boundary layer radiative flux divergencies, a preliminary report.

by

W.H.Moores

Direct measurements of boundary layer radiative flux divergences, a preliminary report

W H MOORES

1. Introduction

During the summer of 1974 the Meteorological Research Unit at Cardington collected data as part of the CABLE experiment. Subsequent analysis of this data has shown that the total heat input into the boundary layer exceeded, by a significant amount (approximately 70 WM^{-2} across a 2 KM deep layer), that transferred by turbulent processes and advective fields. For further details see Moores and Caughey (1977) who argue that this residual energy was radiative in origin.

The radiative contribution to the heat budget of the atmosphere has in recent years been the subject of intensive theoretical study, with particular reference to any climatic effects that aerosol might have, see for example Charlson and Pilat (1969), Braslau and Dave (1973) and Harshvardhan and Hess (1976). Radiative effects are also of importance in the heat budget of the daytime convective boundary layer, for example Glazier, Unsworth and Monteith (1976) and Zobel (1966) have inferred significant warming due to short wave radiation absorption in the lowest 2 KM of the earth's atmosphere. Direct measurements, all of which indicate a radiative warming in the daytime convective boundary layer, have been made by Roach (1961), Murai, Kobayashi, Yamauchi and Goto (1976) and Kondratiev (1961). A recent model of a polluted atmospheric boundary layer, developed by Welch and Zdunkowski (1976) also points to the importance of short wave heating due to aerosol absorption.

Although the existance of short wave absorption in the boundary layer seems to be well documented its absolute magnitude and dependence on atmospheric constituents is uncertain, in particular there is a lack of direct measurements applicable to an area such as Cardington. Because of this and the implication from the CABLE experiment it was decided to investigate the matter further by making radiative measurements at a number of levels simultaneously, using the tethered balloon facility

available at Cardington.

2. Instrumentation

A diagramatic scheme of the experimental arrangement is given in figure 1. The turbulence probes used in this study were the normal 5 component probes without the θ sensor. Further details of the turbulence probe and its method of operation have been given by Caughey (1977). The four signals from the probe (ie T, Q, V and D) and the amplified output (0-3V) from a Funk type net radiometer were input to the telemetry equipment, radioed to the ground and recorded in analogue form on magnetic tape. The Funk radiometers were kindly supplied by Met O 15 and were essentially those used in the fog studies. In addition to the two Funk/turbulence probe pairs an attempt was made to measure the incoming solar radiation and albedo at 1400M using standard Kipp-Zonen solarimeters. Unfortunately the input stages to the amplifiers associated with these solarimeters were prone to pickup resulting in noisy data of poor quality.

This instrumentation was supplemented with the routine surface radiation measurements made at Cardington. Total incoming solar and diffuse solar radiations, in the region 0.3 to 2.5 micron, were measured using unshaded and shaded Kipp-Zonen solarimeters. In addition during the course of the experiment two Kew type radiation balence meters (RBM) were in operation at the surface.

Data of reasonable quality was gathered on six days during the period from the 12th August 1976 to 7th September 1976. In addition to this data comparison runs with the instruments side by side were made on 3 occassions to check for drift in calibration factors. During these ground runs the Funks agreed to within 5 WM^{-2} (1 to 2%). Over averaging periods of 10 minutes the surface radiation balance meter (RBM) agreed with the Funks to within $10WM^{-2}$. The order of the Funks

on the balloon.cable was changed between runs aloft in an attempt to ensure that any net radiation divergence measured was real and not a consequence of the instrumentation.

3. Results

The net radiation measurements for the 6 days of the experiment are given in figures 2-8. All the individual points are 10 minute averages (an average of 60 readings from the Funks and 10 for the RBM). In the data for the 19th August and the 7th September readings from the higher Funk radiometer have been corrected to compensate for a shift in the telemetry zero. The data from figures 2-8 is summarized in table 1 which gives mean values for the net radiation and the radiation divergences. It is convenient to discuss the results in terms of the two atmospheric slabs defined by the instruments. In the following discussion long wave radiation directed away from the earth's surface is positive. Incoming short wave radiation is posative. Net radiation is defined as the excess of incoming over outgoing and a posative net radiation divergence across a slab (net radiation at higher level - net radiation to lower level) gives a warming.

i. Radiation effects in the lowest slab

Except for the period late on the 7th September the net radiation at approximately 150M was higher than that at the surface leading to a radiation absorption, ie a warming in the slab. What is rather surprising is the magnitude of the warming (50 WM^{-2} divergence across a 150M thick slab gives an approximate war ing of $1^{o}C\ hr^{-1}$). This heating is due to the net radiation divergence, it does not indicate which component, ie long or short wave, is responsible for the heating. However, providing temperature and humidity profiles are available the net long wave contribution to the net radiation can be computed using the diagramatic **intergration** techniques outlined by Moëller (1943), Elsasser (1942) and Robinson (1947).

The results of an Elsasser type integration applied to the temperature and humidity profiles measured by the 1100 GMT BALTHUM (the lowest 900M of the atmosphere) and the 1100 GMT Crawley radiosonde ascent (the rest of the atmosphere) on the 20th and 24th August are given in table 2. The 20th and 24th were chosen for an Elsasser type analysis because at around 1100 GMT the net radiation traces (figures 4 and 5) were well behaved (ie no serious interference by low cloud). Table 2 shows that the net long wave is a strong function of the value chosen for the radiative temperature of the earth's surface. On the 20th in particular a 14°C increase in surface temperature causes a long wave radiative cooling of 8 MM^{-2} in the surface to 150M slab to change to a 29MM^{-2} warming. During the experiment, however, no measurements for the radiative temperature of the earth were made. A previous study by Robinson (1950) has shown that, over a short grass surface and in high insolation cases, the surface radiative temperature (T_r) can exceed the screen temperature (T_s) by up to 18°C. An average value from Robinson's data would suggest $T_r = T_s + 7$°C. Work by Jehn (1957) indicates that the surface temperature might be 10–12°C higher than the 4 cms soil temperature. At 1200 GMT on the 20th August the 4 cms soil temperature was 3°C higher than that measured in the screen whereas on the 24th it was 1.5°C lower. If a short wave albedo of 0.2 is taken (see Barry and Chambers 1966) as representative of the rather parched short grass surface that typified Cardington in the dry summer of 1976 use of the total short wave radiation at the surface and output of the RBM at 1100 GMT would suggest a net long wave at 1M of approximately 175MM^{-2} on the 20th and 199MM^{-2} on the 24th, indicative of surface temperatures at least 10°C higher than those measured in the screen (see table 1). These sets of data indicate that the radiative temperature of the earth's surface at 1100 GMT could have easily been 30°C on the 20th and 35°C on the 24th, though such conclusions are clearly tentative.

Taking surface temperatures of 30 and 35°C for the 20th and 24th August and interpolating the values given in table 2 means that in the lowest 150M of the boundary layer the net long wave contribution to the energetics of the slab was a warming of 15WM^{-2} on the 20th and a warming of 32WM^{-2} on the 24th. This compares with the observed net radiation warmings of 48WM^{-2} and 56WM^{-2} on the 20th and 24th and leaves residuals of 33WM^{-2} and 23WM^{-2} to be explained by short wave radiation absorption (plus errors in the techniques and uncertainties in the surface temperature). This inferred value for the short wave absorption in the lowest 150M could certainly be reduced by taking a higher surface radiative temperature.

ii. Net radiation divergence across the top slab

Here again all six days exhibit a marked radiation warming in this 1100M thick slab. Table 2 shows that the net longwave contribution was a cooling of 12WM^{-2} and 30WM^{-2} (using the surface temperatures of 30°C and 35°C derived earlier) for the 20th and 24th respectively. These long wave radiative coolings are strictly applicable to data gathered around 1100 GMT. However, if they are representative of a much longer time period the short wave heatings in this 1100M slab must amount to 54WM^{-2} and 93WM^{-2} for the two days, figures which are surprisingly large.

4. Spatial representively effects

The discussion in the previous section has assumed that radiation effects do not vary in the horizontal. If there is any such variation the net radiation readings from the three heights will exhibit differing degrees of spatial representivity. This is best illustrated by considering the radiation either emitted or reflected at the surface of the earth. The RBM is situated 1M above an extensive short grass surface therefore the upward radiation is representative of just this surface. At higher levels the instruments detect upward radiation representative of a more varied surface type ie concrete, buildings, grass etc. Any such representivity effects are going to be

particularly important in the surface to 150M slab and could help explain why such a large inferred short wave absorption (approx 30WM^{-2}) was necessary to get balance in the layer. It is felt however that the radiometer at 150M is representative of the Cardington area and that the results quoted for the top slab are realistic.

5. Calculations of short wave effects

The calculations presented in this section demonstrate that the inferred short wave absorptions of 54 and 93WM^{-2} across the 1100M thick slab for the 20th and 24th are theoretically reasonable. Because short wave radiation is transmitted downwards through the atmosphere any comprehensive theoretical calculation of its effect in the boundary layer should include the absorption and scattering processes occuring at higher levels. Such a calculation obviously requires a multi-level model. Rather than adopt this complicated and time consuming approach it will be assumed here that the solar radiation reaching the top net radiometer is some fraction, A, of the radiation at the top of the atmosphere. Furthermore it will be assumed that i) the sun radiates as a block body with an effective temperature of 5750°K, ii) the energy distribution is described by Planck's formalism and iii) that A is independent of wavelength. These rather crude assumptions can easily be improved but it is considered that, because of uncertainties inherent in the description of the aerosol, such refinements are unwarranted.

It is possible to obtain a rough estimate for A. The direct solar radiation (I_s) on a surface parallel to the earth can be obtained by taking the diffuse solar radiation from the total solar radiation. The solar radiation incident upon a surface at the top of the atmosphere which is parallel to the earth is given by $I_o \sin\alpha$ where I_o is 1350WM^{-2} and α is the angle of elevation of the sun at a given time. To a crude approximation

$$I_s = AIo \sin\alpha \quad \exp[-\beta_{ext} l']$$ (inferior position as previously)

where L' is the slant range from the surface to top radiometer ($1250M/\sin\alpha$) and β_{ext} is an average extinction coefficient. A plot of $I_s/I_o \sin\alpha$ against L' enables A to be determined. These plots are scattered but suggest a values for A and β of roughly 0.6 and $0.15KM^{-1}$ respectively.

Having estimated the radiation at 1250M it is necessary to make further assumptions before the absorption can be calculated as a function of aerosol concentration. In particular the nature and distribution of the aerosol, throughout the depth of the boundary layer, have to be defined. Clearly this is impossible to do with any degree of certainty however the results given later are based upon the reasonable assumptions that:

i. the aerosol is carbon based with refractive index of 1.8-0.5i. Twitty and Weinman (1971) have given this an an average experimental value for carbon in a number of allotropic forms. Their work should be consulted for more details.

ii. the aerosol distribution is independent of height. Two distributions are used here. They are the ones given by Twitty and Weinman (1971) and are with r, the particle radius, in microns

a) $$n(r) = 5.34\times10^{9}\left(\frac{r}{0.07}\right)^{10}\exp\left[-5\left(\frac{r}{0.07}\right)^{2}\right] + 6.55\times10^{7}\left(\frac{r}{0.07}\right)^{2}\exp\left[-4\left(\frac{r}{0.07}\right)^{\frac{1}{2}}\right]$$

b) $$\begin{aligned} n(r) &= 10^{7} && r < 0.006 \\ &= 400/r^{2} && 0.006 < r < 0.05 \\ &= (1.6\times10^{5})/r^{4} && 0.05 < r < 2 \\ &= 0 && r > 2 \end{aligned}$$

The essential difference in the two distributions is that (b) has many small particles. Following Twitty and Weinman both distributions are normalised to have the same number of particles in the size region $0.07 < r < 2$. The concentration of aerosol is varied by changing this normalization factor

within the limits of 200-2000 particles cms^{-3}. Both distributions are truncated at $r = 10^{-5}$ and r=10.

iii. single particle Mic scattering theory is sufficient to account for the exchanges occuring in a single slab 1100M thick.

iv. the absorption occurs in the solar wavelength region of 0.3 to 5 micron. The integration over the solar spectrum is done in steps of 0.02 microns.

Curves 1 and 2 of figure 9 (aerosol distributions a and b respectively) show the theoretical short wave absorption for a 1100M thick slab based on these assumptions. The plotted data is for 1200 GMT on the 24th August. It is found, however, that the absorption varies by only 2% in the time interval 1000 to 1600 GMT and that it falls by only 3% over the period from the 12th August to the 7th September, ie these curves are valid throughout the experimental period.

The only experimental measurements of aerosol concentration made at Cardington are given in table 1. These surface smoke concentrations, made on behalf of Warren Spring Laboratory, are obtained by drawing a measured volume of air over a 24 hour period through a filter paper. The smoke concentration is then inferred from the darkness of the resulting stain. According to the Warren Spring Laboratory the values quoted in table 1 are probably half the actual low level smoke concentrations. It is still necessary to relate these smoke concentrations, in micrograms M^{-3}, to those given in figure 9. The density of airborne carbon aerosol is likely to be very variable depending upon its form (0.3 - 2.0 gms cms^{-3}). Assuming an aerodynamic density of 1 and a 100% underestimation in the smoke concentrations given in table 1, the theoretical short wave absorption in the 1100M thick slab are $40WM^{-2}$ ($63WM^{-2}$) and $64WM^{-2}$ ($99WM^{-2}$) for the 20th and 24th respectively (the bracketed figure refers to distribution b). These values compare favourably with the values of $54WM^{-2}$ and $93WM^{-2}$ inferred in

section 3.

The assumptions regarding the nature and properties of the aerosol are perhaps the most difficult to justify. These calculations, like those of Twitty and Weinman assume a carbon based aerosol with a refractive index of 1.8 - 0.5i. In an urban atmosphere it is likely that significant amounts of aerosol are combustion products with a high carbon content. Direct evidence for this has been given by Cartwright et al (1956). This is also supported by the mean summer (April to September) smoke converti concentrations for 1974 tabulated by Warren Spring Laboratory. Places like the Outer Hebrides, the Lake District, the South West and the isolated parts of Wales averaging between 1 and 4 micrograms M^{-3} compared with 8 micrograms M^{-3} at Cardington and 20-30 for large cities. Combustion products however can not be the only aerosols present. Hanel (1968, 1971) has discussed how the absorption properties of hygroscopic aerosols depend upon relative humidity. At relative humidities of between 30 and 40%, typical values recorded around midday during this experimental period, he finds a refractive index for aerosol of 1.6-0.02i is valid for particles greater than 0.1 micron in diameter in the wavelength region from 0.3-0.8 micron. Curves 3 and 4 of figure 9 (size distributions a and b) are based on a refractive index of 1.8 - 0.05i which is much nearer the value quoted by Hanel. As would be expected the absorption, for a given concentration, in a 1100M slab is much smaller than that obtained using the average experimental refractive index for carbon, it is however still substantial.

A true urban aerosol is probably a mixture of combustion products and ionic salts together with gaseous pollutants such as NO_2 and SO_2. The absence of any direct measurements of i) the concentration of these species ii) the particle size distributions and iii) how these concentrations and distributions vary as a function of height make the results of any ab-initio

calculation of short wave absorption rather uncertain. However the calculations reported here tend to indicate that the short wave absorptions inferred in section 3 are theoretically possible.

6. Conclusions

The experimental results given here suggest the importance of short wave absorption in the heat budget of the convective boundary layer but leave a few points unanswered. In an attempt to resolve some of the uncertainties a similar experiment is to be undertaken in the summer of 1977. During this experiment it is hoped to directly measure the short wave absorption, to estimate the radiative temperature of the surface of the earth and to measure the albedo at two heights. This will hopefully enable

i. a complete breakdown of the radiation budget in the boundary layer to be made.

ii. the relative importance of turbulent processes and radiative effects as heating mechanisims to be determined.

iii. a relationship between the surface smoke concentration and short wave absorption to be defined.

TABLE 1

DATE	TIME PERIOD (GMT)	AVERAGE NET RADIATION AT 1 M (WM^{-2})	AVERAGE NET RADIATION LOWER FUNKE (HT IN BRACKETS)	AVERAGE NET RADIATION HIGHER FUNKE (HT IN BRACKETS)	AVERAGE LOWER FUNKE - SURFACE (WM^{-2})	AVERAGE HIGHER FUNKE - LOWER FUNKE (WM^{-2})	SMOKE SURFACE CONCENTRATION (M^{-3})	SURFACE VISIBILITY AT 1200 GMT
12 AUGUST	1120 - 1150	289	340 (150M)	380 (1230M)	51	40	23	7KM
19 AUGUST	1150 - 1350	399	463 (150M)	496 (1230M)	64	33	7	15KM
20 AUGUST	1030 - 1320	374	422 (150M)	466 (1230M)	48	44	10	8KM
24 AUGUST	1105 - 1355	333 (RBM 1) 344 (RBM 2)	395 (150M)	458 (1230M)	56	63	16	12KM
26 AUGUST	1220 - 1420	332	368 (150M)	383 (1140M)	36	15	16	12KM
7 SEPT	1310 - 1600	217	302 (60M)	342 (1140M)	85	40	23	13KM
7 SEPT	1615 - 1700	45	25 (60M)	35 (1140)	-20	10	23	

TABLE 2

NET LONG WAVE VALUES (FROM ELSASSER RADIATION CHART)

DATE	SURFACE TEMPERATURE °C	AT HT OF RBM WM^{-2}	AT HEIGHT OF LOWEST FUNKE WM^{-2}	AT HEIGHT OF HIGHEST FUNKE WM^{-2}
20th AUGUST	21.1 (OBSERVED 1M TEMP)	124	132	151
	25.0	144	142	158
	35.0	193	164	172
24th AUGUST	25.9 (OBSERVED 1M TEMP)	125	125	159
	30.0	143	134	164
	40.0	201	146	176

List of figures

Figure 1 — Instrumentation

Figures 2–8 — Net radiation measurements at 3 levels

. higher Funk radiometer
\+ lower Funk radiometer
x surface RBM

Hourly cloud observations are recorded on the abscissa
The dashed line in figure 5 is for the second RBM

Figure 9 — Absorption in a 1100M thick slab as a function of aerosol concentration.

Bibliography

Barry, R G and R Chambers — 1966 — Albedo variations in southern Hampshire and Dorset. Weather 21 60-65

Braslau, N and Dave, J V — 1973 — Effect of aerosols on the transfer of solar energy through realistic model atmospheres. J Appl Met 16 601

Cartwright, J G Nagelschmidt and J W Skidmore — 1956 — The study of air pollution with the election microscope. Quart J Roy Met Soc 82 82-86

Caughey, S J — 1977 — The Cardington turbulence instrumentation TDN 82 Unpublished Met Office note

Charlson, R J and M J Pilot — 1969 — Climate: the influence of aerosols J Appl Met 8 1001-1002

Elsasser, W M — 1942 — Heat transfer by infrared radiation in the atmosphere. Harvard meteor Stud no 6

Glazier J J L Monteith and M H Unsworth — 1976 — Effects of aerosol on the local heat budget of the lower atmosphere Quart J Roy Met Soc 102 95-102

Hanel, G — 1968 — The real part of the mean complex refractive index and the mean density of samples of atmospheric aerosols. Tellus 20 371-379

Hanel, G — 1971 — New results concerning the dependence of visibility on relative humidity and their signifinance in a model for visibility forecast. Beitr Phys Atmos. 44 137-167

Harshvardhan and R D Hess — 1976 — Statospheric aerosol: effect upon temperature and global climate. Tellus 28 1-10

Jehn, K H — 1957 — "Exploring the atmosphere's first mile" edited by H H Lettau and B Davidson - Pergamon Press

Kondratiev, K J — 1961 — Reports at the symposium on radiation in Vienna. Leningrad Univ. English translation

Modeller, F — 1943 — Das Strahlungsdiagramm Wiss Abh DR Reich Wetterd

Moores, W H and S J Caughey — 1977 — A spatial comparison of boundary layer development and heat flux over SE England in anticyclonic conditions. TDN75 Unpublished Met Office note

Murai, K, M Kobayashi T Yamauchi and R Goto — 1976 — The absorption of solar radiation in the lower atmosphere. Papers in Meteorology and Geophysics 27 21-32

Robinson, G D — 1947 — Quart J Roy Met Soc 73 127

Robinson, G D — 1950 — Notes on the measurement and estimation of atmospheric radiation. Quart J Roy Met Soc 76 37-51

Roach, W T — 1961 — Some aircraft observations of fluxes of solar radiation in the atmosphere. Quart J Roy Met Soc 87 346-363

Twitty, J T and J A Weinman — 1971 — Radiative properties of carbonaceous aerosols J Appl Met 10 725-731

Welch, R and W Zdunkowski — 1976 — A radiation model of the polluted atmospheric boundary layer. J Atms Sci 33 2170-2184

Zobel, R F — 1966 — Temperature and humidity changes in the lowest few thousand feet of the atmosphere during a fine summer day in Southern England. Quart J Roy Met Soc 92 196-209

INSTRUMENTATION

FIG 1

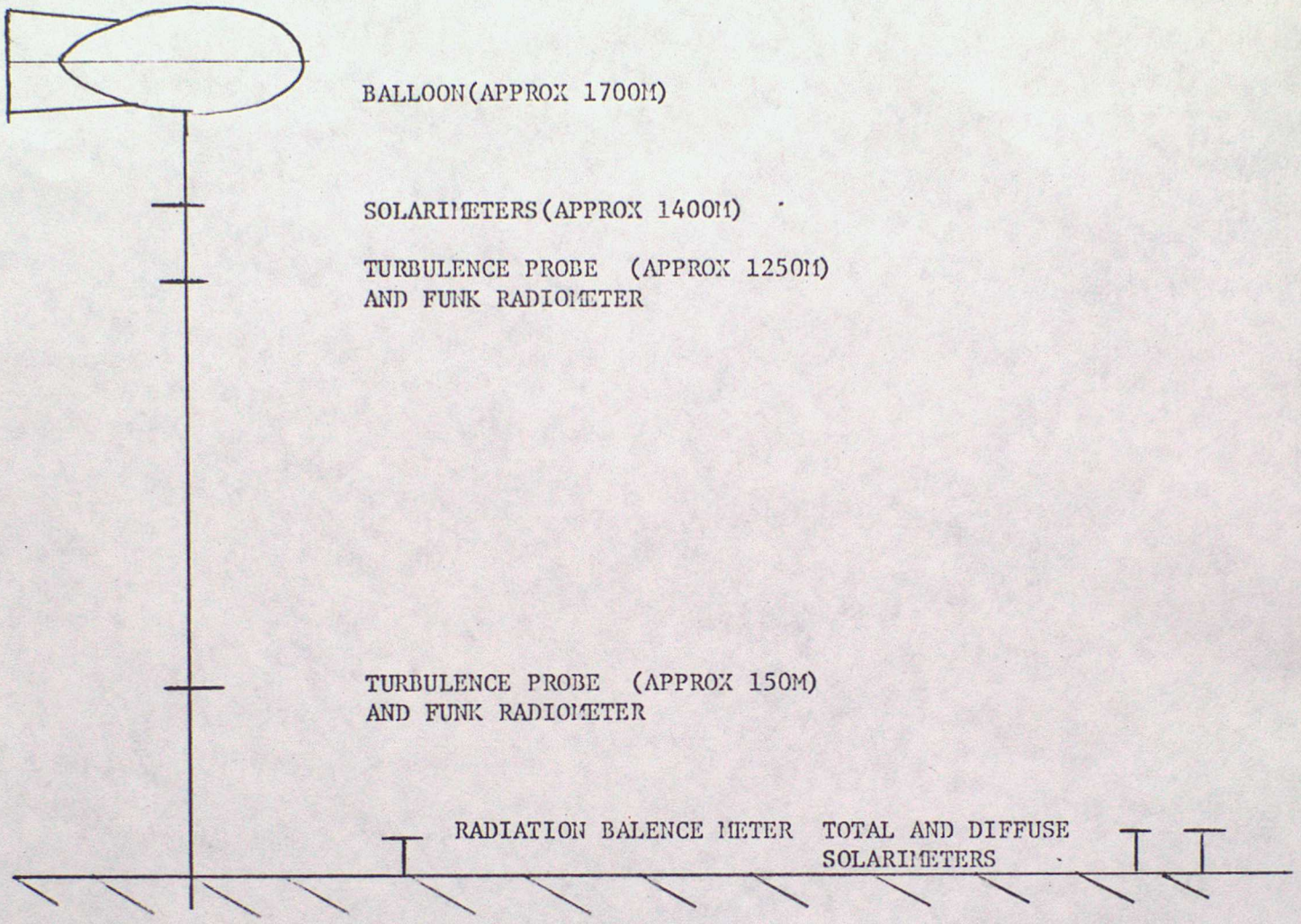

NET RADIATION 12 AUGUST 1976

FIG 2

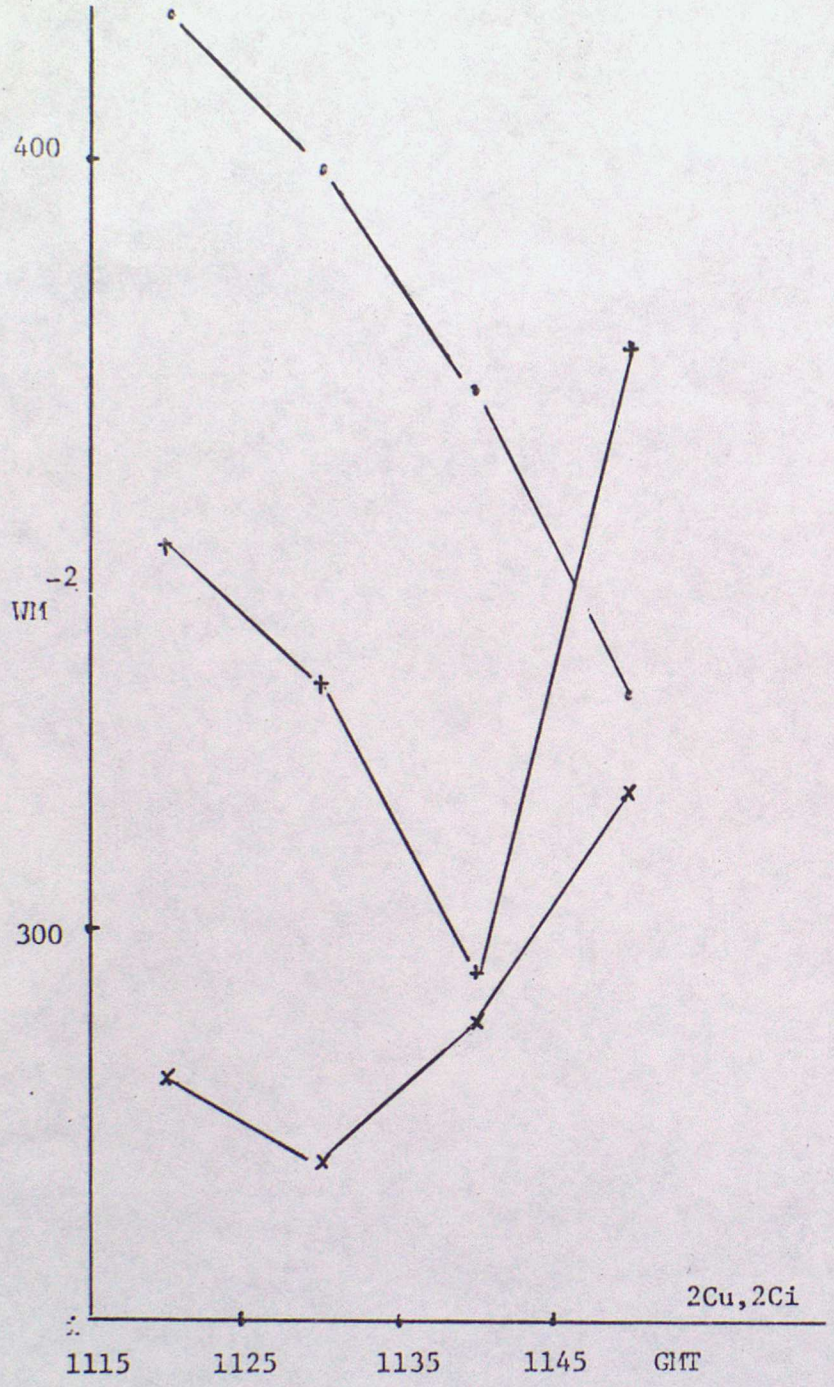

NET RADIATION 19 AUGUST 1976 FIG 3

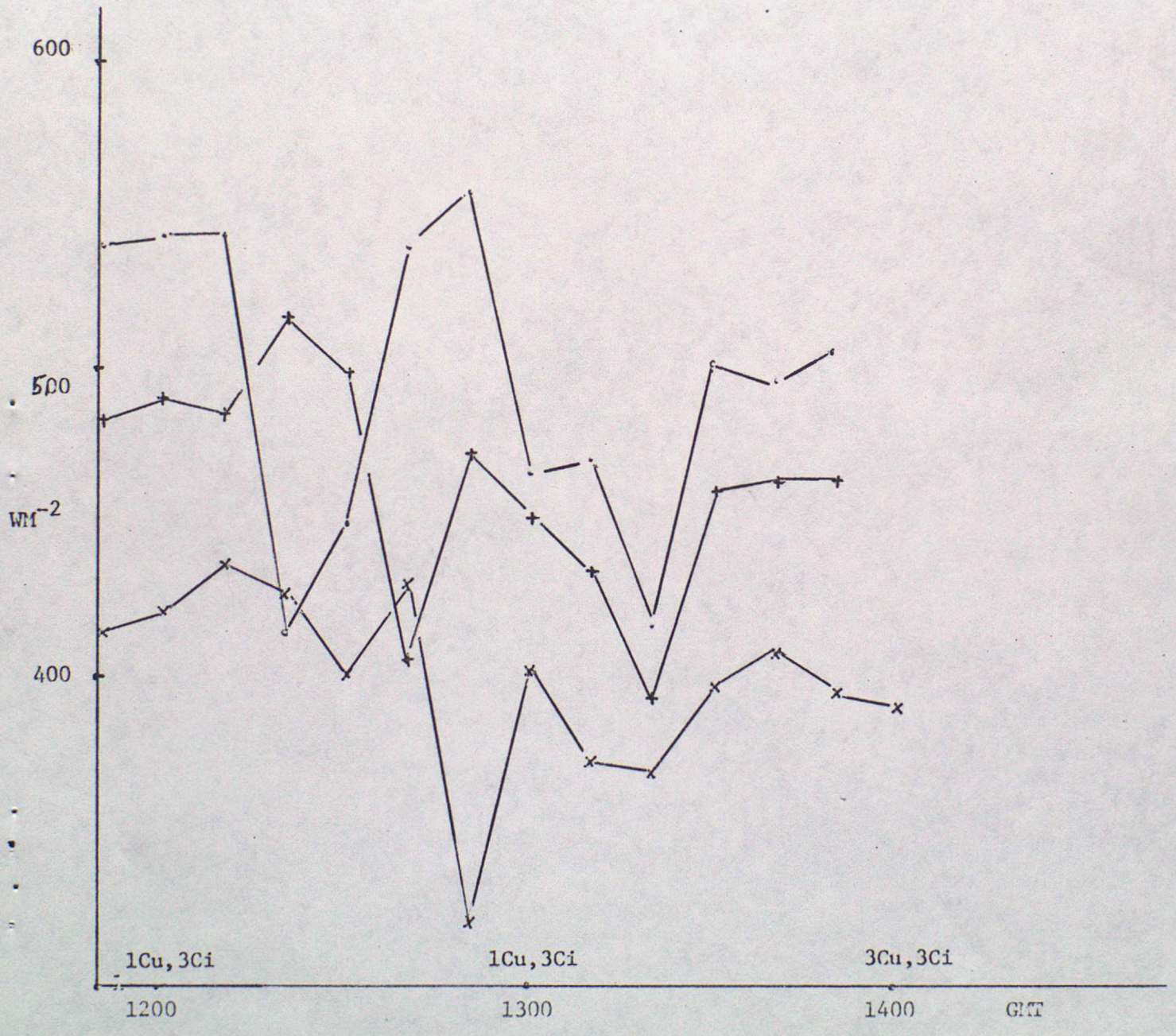

NET RADIATION 20 AUGUST 1976

FIG 4

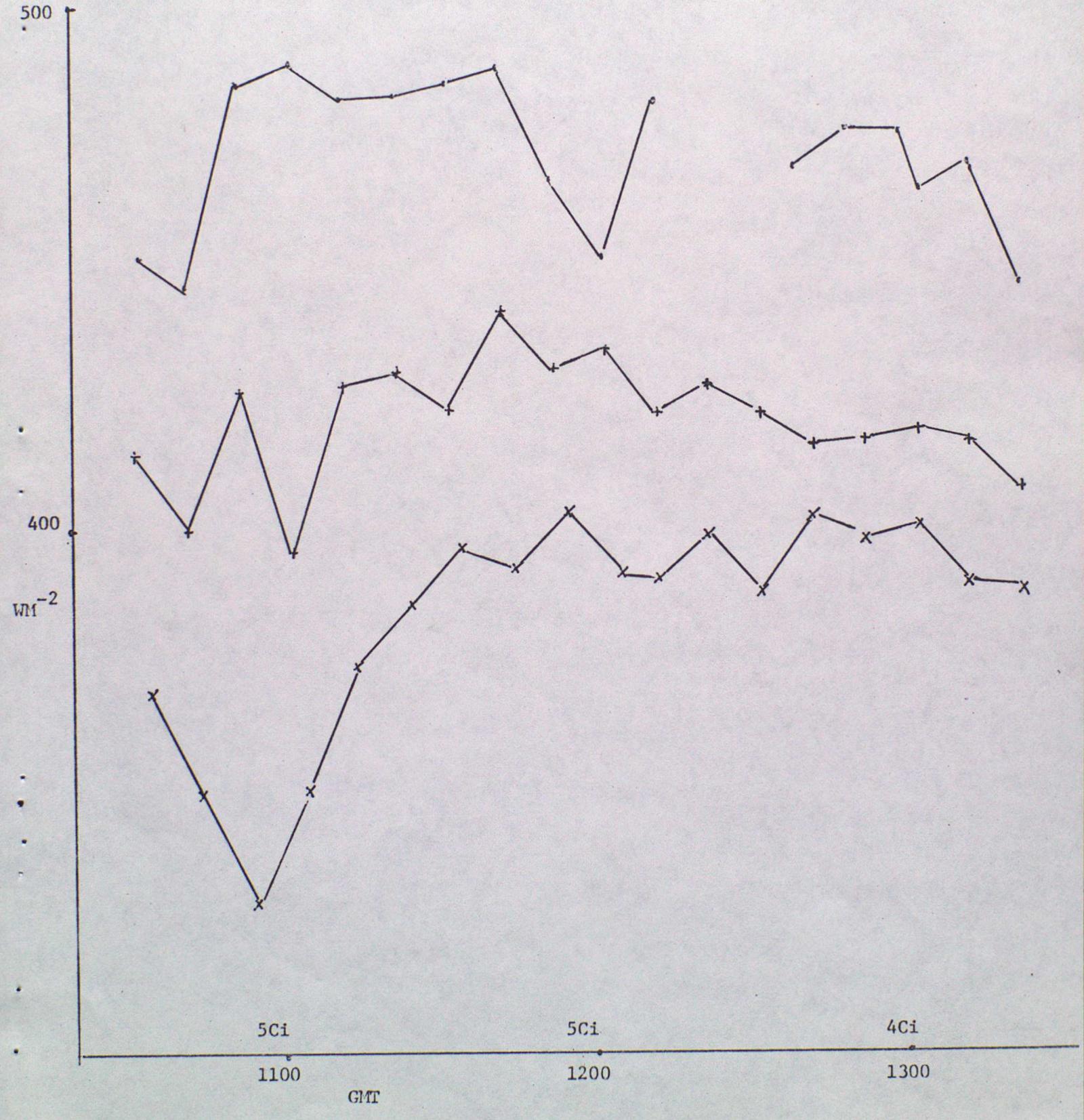

NET RADIATION 24 AUGUST 1976 FIG 5

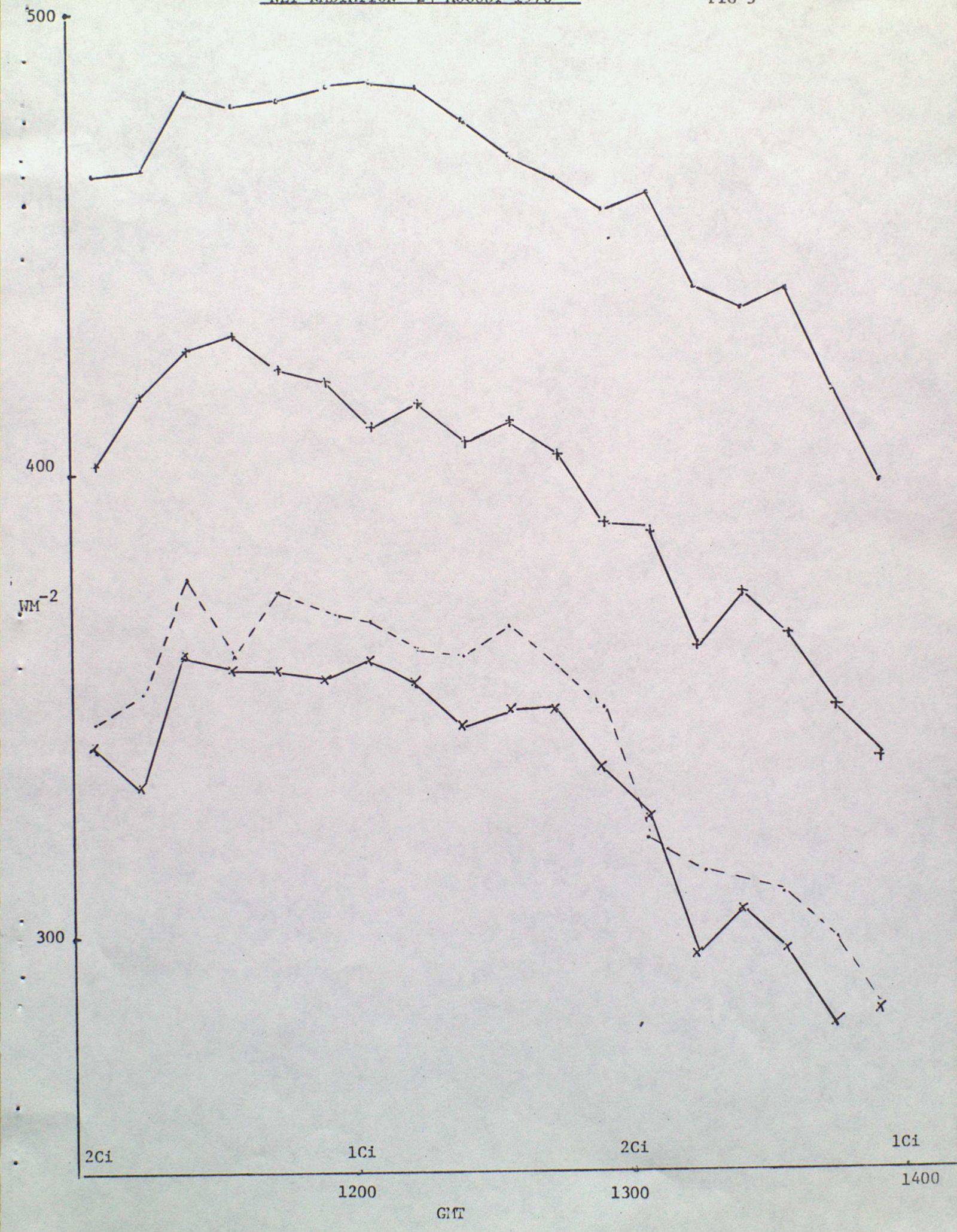

NET RADIATION 26 AUGUST 1976

FIG 6

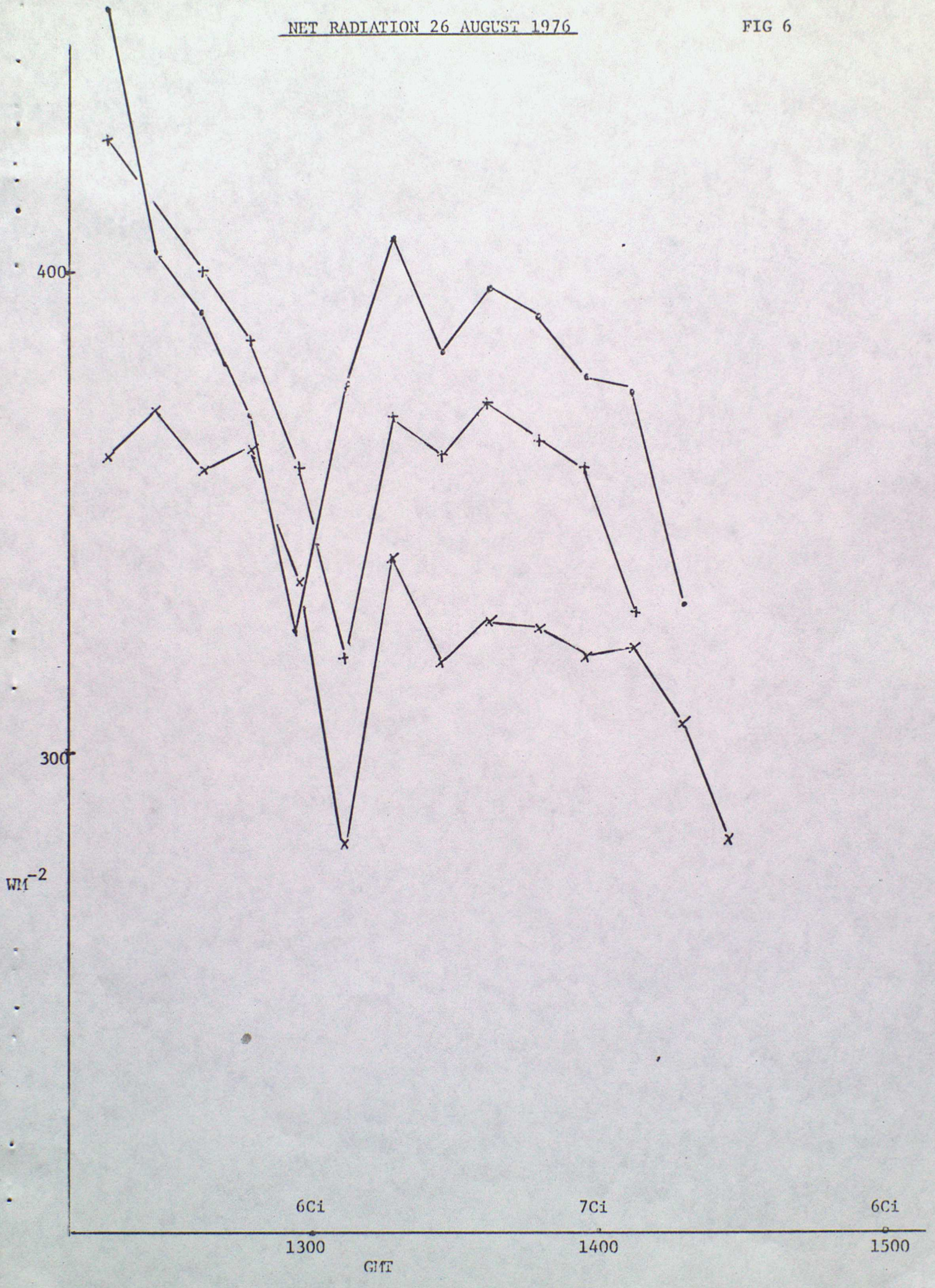

NET RADIATION 7 SEPTEMBER 1976 FIG 7

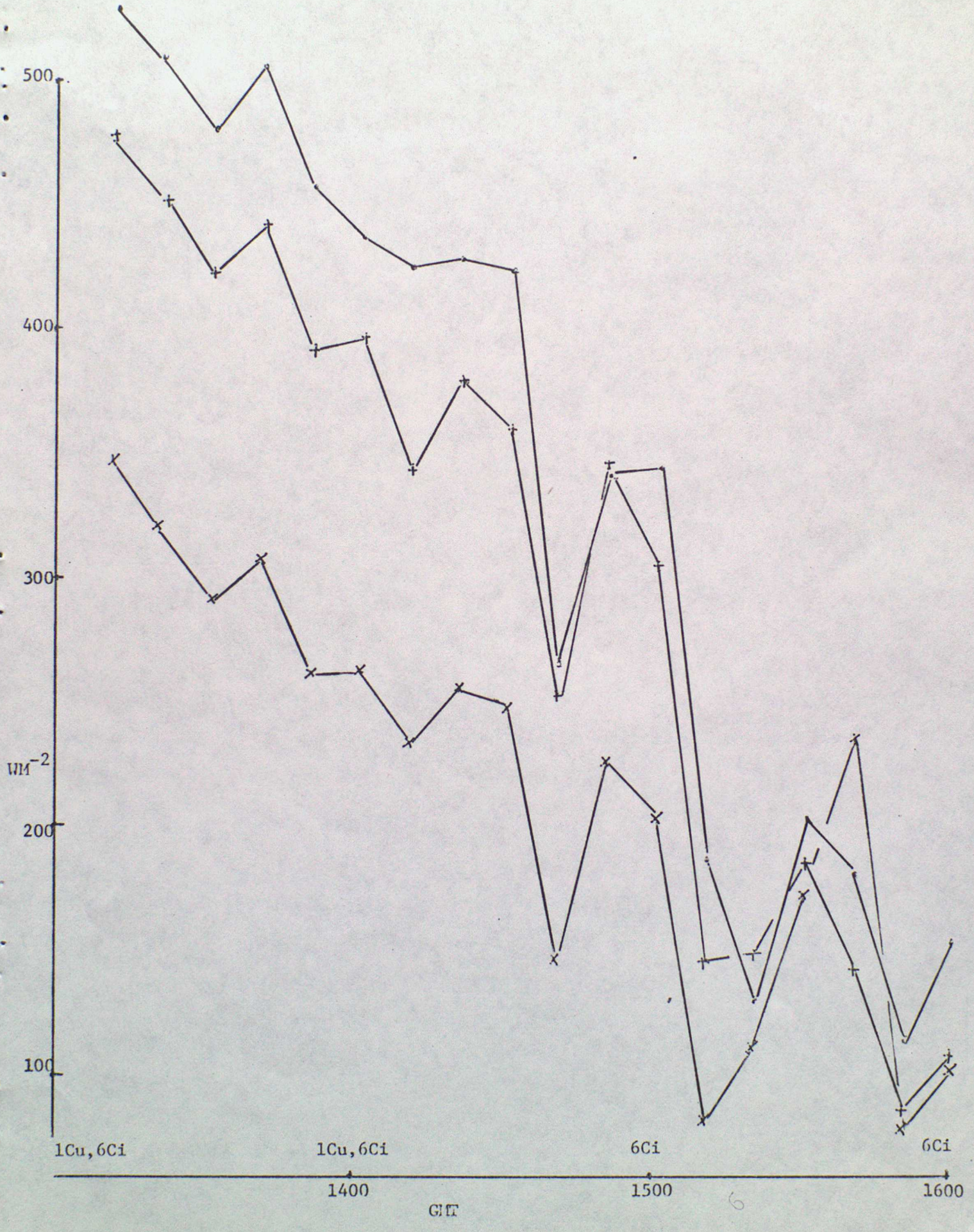

NET RADIATION 7 SEPTEMBER 1976 FIG 8

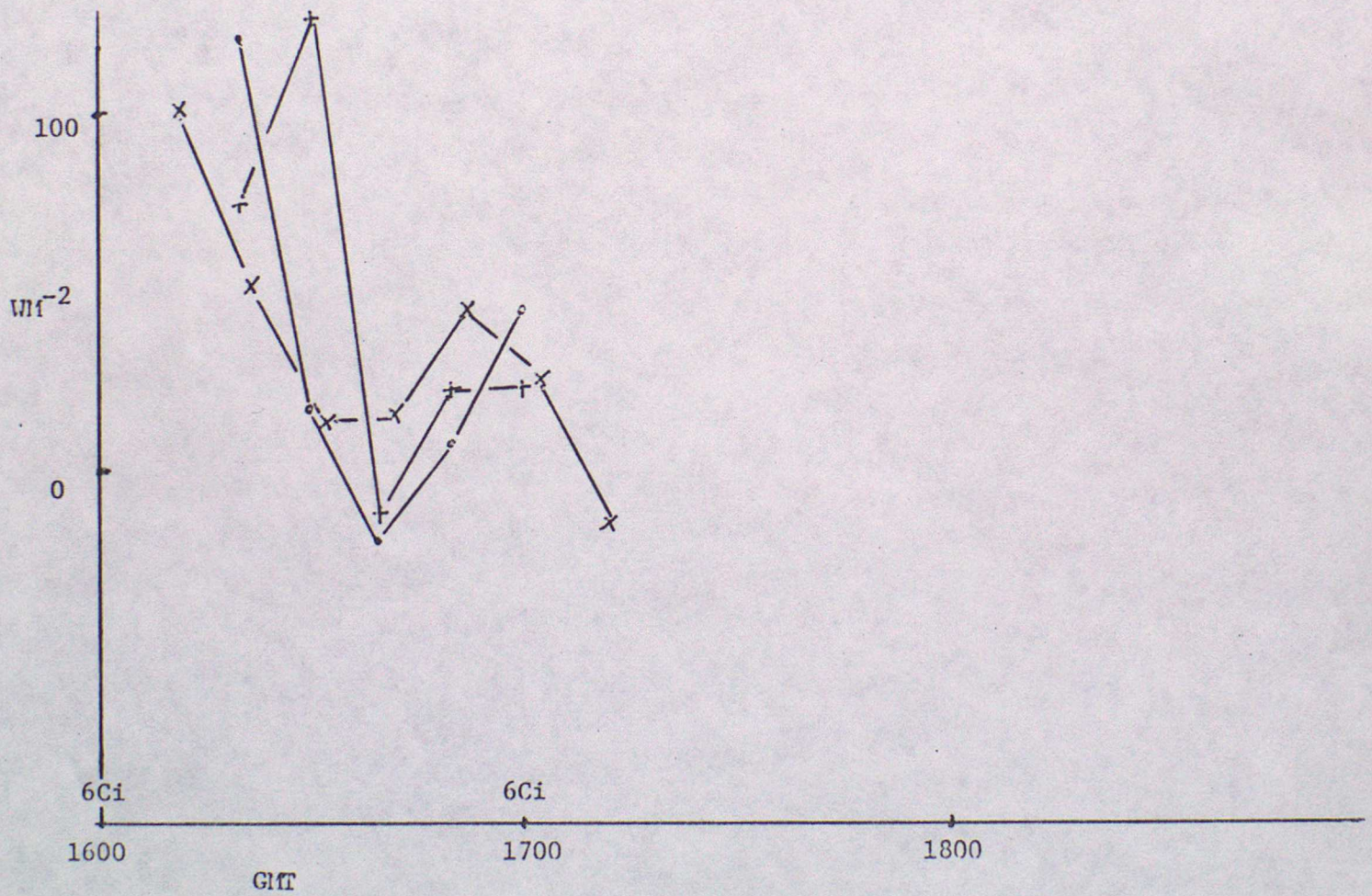

ABSORPTION IN A 1100M THICK SLAB AS A FUNCTION OF AEROSOL CONCENTRATION

FIG 9

1. Aerosol refractive index 1.8-0.5i distribution a
2. Aerosol refractive index 1.8-0.5i distribution b
3. Aerosol refractive index 1.8-0.05i distribution a
4. Aerosol refractive index 1.8-0.05i distribution b